 Bull. Chem. Soc. Jpn. Vol. 83, No. 4, 391–400 (2010)

Crystal Structures of Two Vancomycin Complexes with Phosphate and *N*-Acetyl–D-Ala. Structural Comparison between Low-Affinity and High-Affinity Ligand Complexes of Vancomycin

Takanori Kikuchi,[1] Shyam Karki,[1] Ikuhide Fujisawa,[1] Yoshitaka Matsushima,[2] Yasushi Nitanai,[3] and Katsuyuki Aoki*[1]

[1]Department of Materials Science, Toyohashi University of Technology, Tempaku-cho, Toyohashi 441-8580

[2]Department of Chemistry, Hamamatsu University School of Medicine, Handayama, Hamamatsu 431-3192

[3]Structural Biophysics Laboratory, RIKEN SPring-8 Center, Harima Institute, 1-1-1 Kouto, Sayo-gun, Hyogo 679-5148

Received December 9, 2009; E-mail: kaoki@tutms.tut.ac.jp

Crystal structures of two vancomycin complexes with phosphate and *N*-acetyl–D-Ala (AcDA) were determined. Each complex involves two crystallographically independent vancomycin molecules (V1 and V2) in the asymmetric unit, which form a usually observed back-to-back arranged vancomycin dimer V1–V2 with two disaccharide chains packed in a head-to-head manner, but only one of the two ligand-binding sites is occupied. Comparison of the published crystal structures of low-affinity (small in molecular size) ligand complexes of vancomycin with high-affinity (large) ligand complexes reveals that when the high-affinity ligand binds, three structural factors (hydrogen-bonding interactions between the two peptide-backbones and hydrophobic intra-dimer sugar–ring and ring (face)–ring (edge) interactions) work to enhance the stabilization of the back-to-back dimer-interface, an important factor that is believed to promote antibacterial activity. It has also been revealed, by examining the high-affinity ligand complexes (including *N*-acetyl–D-Ala–D-Ala), that sugar–ligand interaction could cause different affinities of the two halves of the dimer; this is a factor responsible for the failure of the ligand binding to V1 in the AcDA complex. Possible scenarios for the formation of vancomycin complexes with low-affinity as well as high-affinity ligands are presented.

Vancomycin (Figure 1), which belongs to a family of glycopeptide antibiotics that are active against gram-positive bacteria, is clinically of special importance because it represents the last line of defense against bacteria that have developed resistance to other antibiotics.[1] However, the recent emergence[2] of vancomycin-resistant bacterial strains has brought a limitation in the treatment of vancomycin and has required prompt development of new therapeutic drugs. Glycopeptide antibiotics function by binding nascent cell-wall disaccharide–pentapeptides terminating in the sequence –D-Ala–D-Ala to inhibit the synthesis of the linkage between mucopeptides, thereby weakening the resulting cell-wall.[3] As the peptide–ligand recognition mechanism, the formation of five hydrogen bonds between an antibiotic and a ligand was proposed from spectroscopic studies[4] and this has indeed been substantiated first in crystal structures of a balhimycin complex[5] with L-Lys–D-Ala–D-Ala, or a degluco-balhimycin complex[5] with L-Ala–D-Glu–γ-L-Lys–D-Ala–D-Ala and subsequently in crystal structures of vancomycin complexes with *N*,*N*′-diacetyl–L-Lys–D-Ala–D-Ala[6] and *N*-acetyl–D-Ala–D-Ala.[6,7]

On the other hand, the –D-Ala–D-Ala terminus is replaced by –D-Ala–D-lactate in vancomycin-resistant strains (VRE)[8] and the affinity of vancomycin for precursor analogs terminating in –D-Ala–D-lactate is decreased by a factor of the order of 1000 relative to the binding to precursors terminating in –D-Ala–D-Ala,[9] corresponding to the low activity of vancomycin against bacteria that biosynthesize such precursors.[10] The drastically reduced binding constants have been assumed[11] to be due to electro-repulsive interaction between the ester oxygen of the C-terminal D-lactate group and the carbonyl oxygen of residue 4 of the antibiotic backbone, which forms a hydrogen bond with the NH of the terminal D-alanine group of the normal precursors. We have verified[6] this O···O repulsion and the concomitant lengthening of two neighboring hydrogen bonds in the crystal structure of a vancomycin complex with *N*,*N*′-diacetyl–L-Lys–D-Ala–D-lactate. In this structure and also in the *N*,*N*′-diacetyl–L-Lys–D-Ala–D-Ala complex, of special interest is an observation that a water molecule bridges the antibiotic molecule to the ligand by forming hydrogen bonds with the carboxylate terminal oxygen of antibiotic and the amide nitrogen of the Lys residue of the ligand. We suggest[6] that this may provide a strategy for designing drugs against VRE: the modification of the C-terminus of the antibiotic to form a direct hydrogen bond with the amide nitrogen of the third residue (Lys) from the C-terminus of the ligand could stabilize the structure of the antibiotic–ligand complex more effectively.

In order to examine the significance of the water-mediated antibiotic–ligand interaction and thus to define a minimal set of interactions necessary for the complex formation with the vancomycin-resistant precursors terminating in –D-Ala–D-lactate, we have now tried the complex formation of vancomycin with *N*-acetyl–D-Ala–D-lactate, yielding two crystalline compounds depending on pH conditions. X-ray diffraction

Published on the web March 26, 2010; doi:10.1246/bcsj.20090326

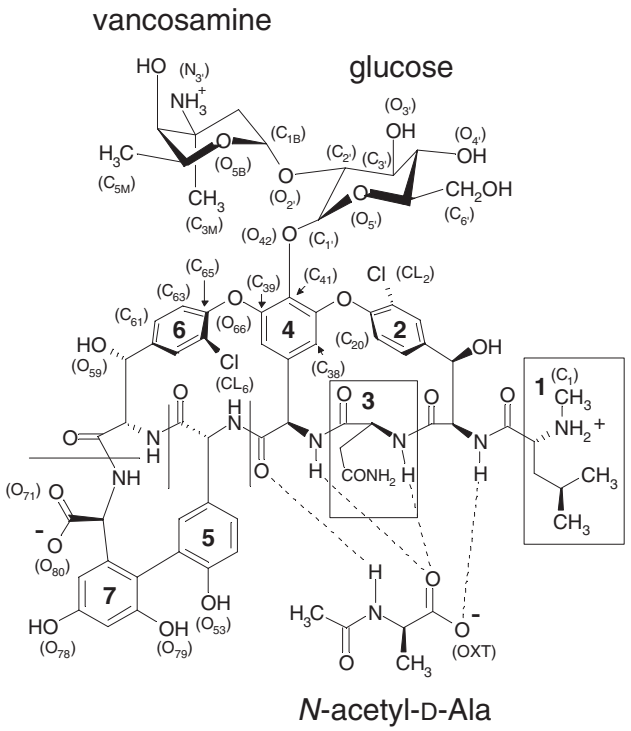

Figure 1. Chemical structure of vancomycin and the binding scheme between vancomycin and a cell-wall precursor analog, *N*-acetyl–D-Ala (AcDA). The amino acid residues of vancomycin are numbered. Atoms mentioned in the text are labeled. The hydrogen bonds between vancomycin and AcDA are shown by broken lines.

analysis has revealed that under nearly neutral pH condition, *N*-acetyl–D-Ala–D-lactate does not bind to antibiotic but instead a phosphate buffer ion occupies the ligand-binding site. On the other hand, under slightly acidic conditions, the hydrolysis of *N*-acetyl–D-Ala–D-lactate took place to give *N*-acetyl–D-Ala (AcDA) that binds to antibiotic. We report here crystal structures of two resulting vancomycin complexes, one being with phosphate (the phosphate complex) and the other with a normal cell-wall precursor analog *N*-acetyl–D-Ala (the AcDA complex with the space group $P4_32_12$). A vancomycin–AcDA complex with a different crystal form (triclinic $P1$) is reported.[12]

In addition, in order to provide further information for our better understanding of ligand-binding effects on vancomycin structures, we here compare so far reported crystal structures of vancomycin complexes,[6,7,12–16] involving those with low-affinity (small in molecular size) ligands such as acetate (OAc),[13,14] *N*-acetylglycine (AcG),[15] D-lactic acid (DLac),[15] and *O*-acetyl-D-lactic acid (AcDLac)[15] and those with high-affinity (large) ligands *N*-acetyl–D-Ala–D-Ala (NAAA)[6,7] and *N*,*N*′-diacetyl–L-Lys–D-Ala–D-Ala (DALAA).[6]

Results and Discussion

Co-crystallization Experiments of Vancomycin with *N*-Acetyl–D-Ala–D-Lactate. A total of thirty different crystallization conditions were examined and two crystalline compounds were obtained. X-ray diffraction analysis has revealed that under phosphate buffer conditions (pH 6.5), *N*-acetyl–D-Ala–D-lactate does not bind to antibiotic, but a phosphate buffer ion occupies the ligand-binding site (the phosphate complex). Under slightly acidic conditions, *N*-acetyl–D-Ala–D-lactate was hydrolyzed and a complex with *N*-acetyl–D-Ala formed (the AcDA complex). This shows that the formation of a stable complex with *N*-acetyl–D-Ala–D-lactate is considerably difficult, suggesting that the ligand affinity of vancomycin for *N*-acetyl–D-Ala–D-lactate may be little and, at least less than that for phosphate. It may be reasonable to assume that the stabilization by the possible hydrogen-bonding, when *N*-acetyl–D-Ala–D-lactate binds to antibiotic, between the amide nitrogen of the seventh residue of the antibiotic backbone and the acetyl oxygen of the ligand is not enough to compensate for electrostatic repulsion that could occur between the ester oxygen of ligand and the carbonyl oxygen of residue 4. On the other hand, the binding of the phosphate ligand is achieved by the formation of a P–O–H (ligand)···O (the carbonyl oxygen of residue 4) hydrogen bond in addition to three other conventional hydrogen bonds, as described later in detail. We propose here that since *N*,*N*′-diacetyl–L-Lys–D-Ala–D-lactate does bind to the antibiotic,[6] the third Lys residue from the C-terminus of the ligand might be necessary as a minimal set for the formation of a stable complex with vancomycin-resistent precursors terminating in –D-Ala–D-lactate, that is, the formation of the water-mediated N–H (amide of the third residue of ligand)···water···O (carboxylate oxygen of residue 7) hydrogen bonds[6] is required for the complex formation.

Overall Structures of the Phosphate and AcDA Complexes. The nomenclature is adopted by that of Loll et al.[13] with modifications where necessary. In both the phosphate and AcDA complexes, the asymmetric unit contains two vancomycin molecules, referred to herein as V1 and V2. The seven amino acid residues of vancomycin are denoted as V1:1 to V1:7 and V2:1 to V2:7. When the backbone atoms of the antibiotic or the ligand are mentioned, N, C_α, C, or O are used (e.g., "V1:2 N" denotes the amide nitrogen atom of the second residue of V1). The glucose and vancosamine sugars on each monomer are indicated as "Glu" and "Van," respectively. Other atoms are referred to as the names shown in Figure 1.

Structures of the present phosphate and AcDA complexes are isomorphous with the vancomycin complexes with low-affinity ligands such as OAc,[13,14] AcG,[15] DLac,[15] and AcDLac,[15] which exclusively crystallized in the tetragonal space group $P4_32_12$ and share common structural as well as crystal packing features to one another. Hence, the asymmetric unit contains a back-to-back arranged vancomycin dimer V1–V2 with two disaccharide chains packed in a head-to-head manner, and only one of the two ligand-binding pockets is occupied by a ligand molecule in V2, as shown in Figure 2 (for the phosphate (2a) and AcDA (2b) complexes), where the vancosamine sugar lies over the ligand-binding pocket in V1, while glucose locates at the corresponding position in V2.

Structures of Back-to-Back Arranged Dimers. It has been well documented,[1] based mainly on NMR studies, that glycopeptide antibiotics have a strong propensity to form a back-to-back-dimer through four hydrogen bonds between two aglycons in an anti-parallel arrangement. This has indeed been repeatedly exemplified in crystal structures of vancomycin,[6,7,12–16] aglycovancomycin,[17] A-40926 aglycone,[18]

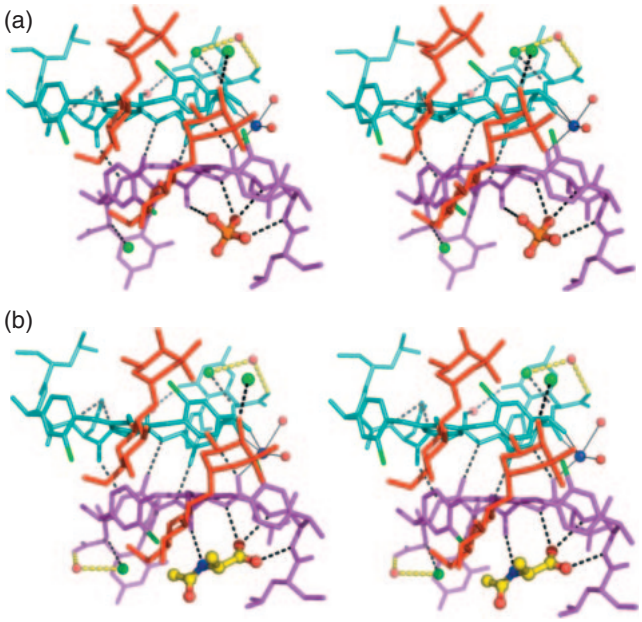

Figure 2. Stereoviews of asymmetric units in vancomycin complexes. (a) The phosphate complex. (b) The AcDA complex. Vancomycin molecules are represented as stick models, and ligands are represented as ball-and-stick models. The sugar moieties of vancomycin molecules are represented as red sticks. Chlorine atoms or chloride ions are drawn with green in color and sodium ions are with violet. Red spheres represent water molecules. Hydrogen bonds are depicted by dotted lines.

balhimycin,[5,19] degluco-balhimycin,[5] ureidobalhimycin,[20] and decaplanine,[21] and this is also the case for the present phosphate and AcDA complexes of vancomycin. Exceptions are monomeric degradation products such as the CDP-1 analog of vancomycin[22] and the CDP-1 analog of methylated vancomycin.[23]

Antibiotic back-to-back arranged dimerization is believed[24] to promote antibacterial action because the binding of one monomer to the bacterial cell wall brings a second monomer into proximity with other peptidoglycan ligands to form a chelate with the peptidoglycan. For this action, the stabilization of the dimer structure is of primary importance. It is also known[1] that the dimerization is cooperative with ligand binding. We point out that the following four structural factors could stabilize the dimer-interface: (**i**) hydrogen-bonding interactions between the two peptide-backbones,[1] (**ii**) interactions between two disaccharide chains,[13] (**iii**) hydrophobic interactions between sugars of disaccharides and cross-linked aromatic side chains of residues 2 or 6 across the dimer-interface, and (**iv**) edge-to-face ring–ring interactions between cross-linked aromatic side chains of residues 4 and 6.[13] We here examine which structural factors could affect the tightness of the dimer-interface when ligand binds to antibiotic, based on the known crystal structures of vancomycin complexes, including the present work.

(**i**) Table 1 lists hydrogen-bonding distances between the two peptide-backbones at the dimer-interface. It appears that the distances of two chemically equivalent outer hydrogen-bonds [V1:3 O···V2:6 N (**a** in Table 1) and V1:6 N···V2:3 O (**d**)] are

Table 1. Hydrogen-Bonding Distances (Å) at the Back-to-Back Dimer-Interface in the Vancomycin Complexes

Ligand	V1:3 O···V2:6 N (**a**)	V1:5 N···V2:5 O (**b**)	V1:5 O···V2:5 N (**c**)	V1:6 N···V2:3 O (**d**)	PDB code	CCDC code	Ref.
OAc	3.14	2.91	2.87	3.05	1AA5		13
AcG	3.17	2.95	2.87	3.09	1QD8		15
DLac	3.11	2.91	2.84	3.07	1C0R		15
AcDLac	3.13	2.92	2.85	3.05	1C0Q		15
Phosphate	3.05	2.90	2.81	3.03		728179	this work
AcDA	3.13	2.91	2.81	3.02		728180	this work
Cu^{2+} ion	2.90	2.85	2.96	3.02		655637	16
NAAA[a)]	3.11	2.81	2.87	3.19		693248	6
DALAA[b)]	3.16	2.80	2.86	3.23	1FVM		6
DALALac[c)]	3.18	2.82	2.86	3.20		693249	6

a) Average values are given for 3 independent V1–V2 dimers. b) Average values for 2 independent V1–V2 dimers. c) Average values for 2 independent V1–V2 dimers.

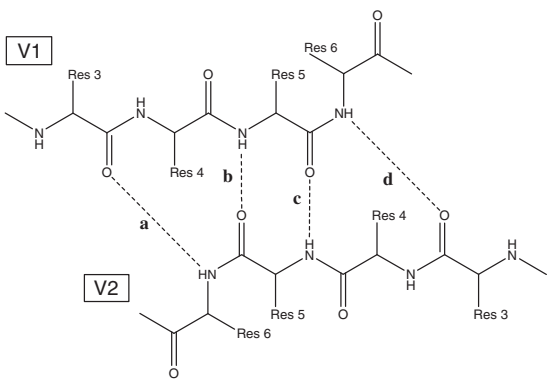

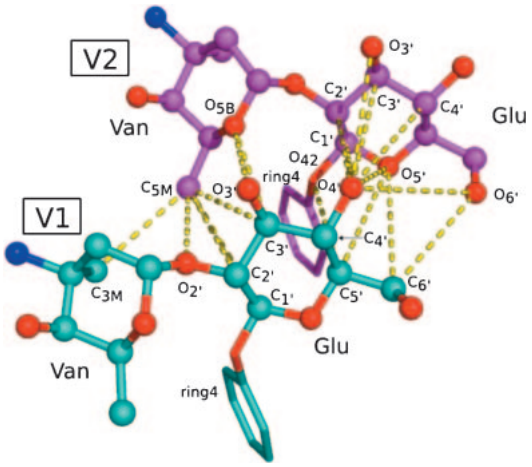

Figure 3. Close contacts (<4.0 Å), drawn with dotted lines, between two parallelly arranged disaccharide chains at the back-to-back dimer-interface in the AcDA complex.

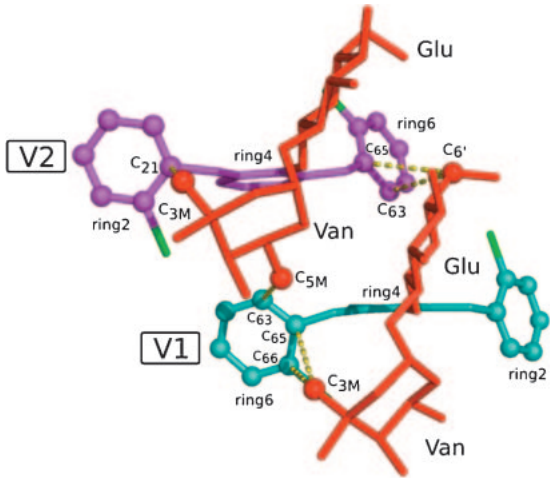

Figure 4. Hydrophobic contacts between sugars and aromatic rings at the back-to-back dimer-interface in the AcDA complex. The sugar–ring closest contacts of two intramolecular and two intermolecular pairs are drawn with dotted lines.

considerably longer (weak) than those of two inner hydrogen-bonds [a pair of V1:5 N···V2:5 O (**b**) and V1:5 O···V2:5 N (**c**)], which fall in the normal values for N–H···O hydrogen-bonds. When the high-affinity ligand binds, the inner hydrogen-bond **b** becomes shorter, while the outer hydrogen-bond **d** becomes longer. The other inner **c** and the other outer **a** hydrogen-bonds are little influenced. Taking into consideration that the long hydrogen-bonding (weak interaction) **d** may exert its minor contribution to the structural stabilization comparing with the shorter hydrogen-bonding **b**, we suspect that as a whole, the binding of the high-affinity ligand somewhat surpasses that of the low-affinity ligand with regard to the dimer stabilization due to hydrogen-bonding interactions between the two peptide-backbones.

(**ii**) Two parallel disaccharide chains make extensive van der Waals contacts with each other, as shown in Figure 3 (and Table S-1 as Supporting Information). Common to all 10 vancomycin complexes, close contacts (<4.0 Å) occur to similar extent between the edge ($O_{4'}$) of V1:Glu and the face of V2:Glu, between the edge (O_{5B}) of V2:Van and the edge ($O_{3'}$ and $C_{3'}$) of V1:Glu, and between the edge (C_{5M}) of V2:Van and the edge ($O_{2'}$ and C_{3M}) of V1:Glu. Among these, very short interatomic distances are observed between the hydroxy $O_{4'}$ of V1:Glu and the ring atom $C_{2'}$ of V2:Glu within the range of 3.41–3.90 Å and between the methyl group C_{5M} of V2:Van and the ether bridge $O_{2'}$ of V1:Glu within the range of 3.40–3.59 Å. Hence, intermolecular sugar–sugar interactions may exert nearly equal contribution to the stabilization of the dimer-interface in these vancomycin complexes.

(**iii**) There are two kinds of sugar–ring hydrophobic interactions, one being intra-monomer and the other intra-dimer (Figure 4 and Table S-2). The former may contribute to stabilize structures of V1 or V2 monomers themselves, while the latter may stabilize the structure of the dimer-interface. Intra-monomer interactions in V1 occur between the methyl substituent C_{3M} of vancosamine and cross-linked aromatic side chain of residue 6, and in V2 between vancosamine C_{3M} and the face of ring 2. Intra-dimer interactions occur at two sites, one between the methyl group C_{5M} of vancosamine of V2 and ring 6 of V1 and the other between the hydroxymethyl $C_{6'}$ of glucose of V1 and ring 6 of V2. It should be noted here that when larger ligands (NAAA and DALAA) bind to antibiotic, the intra-dimer closest contact between C_{5M} of V2 and C_{63} of V1 becomes shorter compared with that for small ligands (OAc, AcG, DLac, AcDLac, phosphate, or AcDA): the average distance of V2:Van C_{5M}···V1:6 C_{63} contact is 3.57 Å [distributed from 3.50 to 3.72 Å] for larger ligands, while the corresponding value is 3.97 Å [with the range of 3.92–4.00 Å] for small ligands. On the other hand, the closest contact between $C_{6'}$ of V1 and C_{63} or C_{65} of V2 becomes somewhat longer when larger ligands bind: the V1:Glu $C_{6'}$···V2:6 C_{63} or C_{65} average distance is 3.79 Å [with the range of 3.64–4.11 Å] for larger ligands while the corresponding average value is 3.60 Å [with the range of 3.49–3.68 Å] for small ligands. As a whole, when the high-affinity ligand binds, the stabilization of the dimer-interface due to sugar–ring hydrophobic contacts may increase to some extent.

(**iv**) Cross-linked aromatic side chain rings 4 and 6 within each monomer are nearly perpendicular to each other (Figure 4 and Figure S-1). At the dimer-interface, there are two sets of edge-to-face π-interactions, one between the face of ring 4 of V1 and the edge (C_{63}) of ring 6 of V2 and the other between the face of ring 4 of V2 and the edge (C_{63}) of ring 6 of V1. Table 2 shows that, when large ligands (NAAA, DALAA, or even DALALac) bind to antibiotic, edge-to-face π-interactions become more effective (stronger) compared to those of small ligands, especially prominent at the C-terminal side of V1 (see V1:6 C_{63}···V2:4 C_{41} distance). This may be, at least in part, due to closer contacts between vancosamine of V2 and the face of ring 6 of V1 for large ligands than for small ligands, as noted in (**iii**), and vice versa.

In summary, when the high-affinity ligand binds, factors (**i**), (**iii**), and (**iv**) work to make the dimer-interface tighten to some extent.

Ligand-Binding Sites. As Figure 2 shows, each vancomycin monomer in the phosphate and AcDA complexes forms

Table 2. Selected Interatomic Distances (Å) around O_{66} Atoms at the Back-to-Back Dimer-Interface, Involving Edge-to-Face Interactions between Cross-Linked Aromatic Rings 4 and 6

Ligand	V1:4 C_{41}··· V2:6 C_{63}	V1: O_{66}··· V2: O_{66}	V1:6 C_{63}··· V2:4 C_{41}	Ref.
OAc	4.06	4.60	4.54	13
AcG	4.17	4.72	4.59	15
DLac	4.06	4.57	4.50	15
AcDLac	4.04	4.61	4.49	15
Phosphate	4.03	4.32	4.31	this work
AcDA	4.05	4.64	4.43	this work
Cu^{2+} ion	3.84	3.92	3.99	16
NAAA[a)]	3.93	4.25	4.12	6
DALAA[b)]	3.93	4.23	4.09	6
DALALac[b)]	3.92	4.34	4.19	6

a) Average values are given for 3 independent V1–V2 dimers.
b) Average values for 2 independent V1–V2 dimers.

an open bowl with the peptide backbone located on the bottom (also shown in Figure S-2 for a V1 monomer and Figure S-3 for V2 monomers). The least-squares fits (performed using the program ProFit[25]) of V1 and V2 monomers gave the rms difference of the fitted atoms of 0.26 Å for the phosphate complex and 0.24 Å for the AcDA complex, when the heptapeptide-backbone atoms involving C^{β} of each vancomycin molecule are compared. This shows that the conformational change on the ligand binding occurs to some extent, reflecting in the width of the entrance of the binding pocket (estimated by the distance between V:7 O_{79} and V:1 C^{γ}; see Figure 1 for the atom numbering): 8.20 Å for V1 and 8.67 Å for V2 in the phosphate complex, and the corresponding distances in the AcDA complex are 8.15 and 8.55 Å. On the other hand, the least-squares fits of V1 in the phosphate complex and V1 in the AcDA complex, and V2 in the phosphate complex and V2 in the AcDA complex are 0.06 and 0.14 Å, respectively, showing no conformational difference between two V1 monomers or minor difference between two V2 monomers. It is of interest to note here that the width of the entrance of the ligand-binding pocket decreases when the ligand becomes larger: OAc[13] [8.78 Å] → AcDA [8.55 Å] → NAAA[6] [7.88 to 8.34 Å (average, 7.99 Å)] → DALAA[6] [7.06 to 8.05 Å (average, 7.59 Å)].

In the structures of V1 monomers in both the phosphate and AcDA complexes, no ligand locates at the binding pocket. Instead, the carbamoyl side-chain group of Asn residue participates in the formation of two intramolecular N–H···O hydrogen bonds with two amide nitrogens V1:3 N and V1:4 N of the peptide backbone: V1:3 N···V1:3 $O^{\delta 1}$ and V1:4 N···V1:3 $O^{\delta 1}$ distances are 2.81 and 2.80 Å, respectively, for the phosphate complex and 2.82 and 2.81 Å for the AcDA complex. Loll et al. suggested[13] that the Asn residue, which is essential for antimicrobial activity,[26] acts as an intramolecular surrogate ligand in the absence of the ligand, thereby promoting the ligand-binding activity by preventing solvation or facilitating desolvation of the binding site.

In the structures of V2 monomers, a phosphate ligand or an AcDA ligand binds to the peptide backbone through four hydrogen bonds, three of which are with amide nitrogens V2:1 N, V2:3 N, and V2:4 N and one with carbonyl oxygen V2:4 O (Figure 2a for the phosphate complex and Figures 1 and 2b for the AcDA complex). Table 3 lists hydrogen-bonding distances between vancomycin and ligand molecules, along with those of other vancomycin complexes whose crystal structures have been determined. The phosphate ligand participates in a weak P–O–H···O (V2:4) hydrogen-bonding in addition to three conventional N–H···O (phosphate) hydrogen bonds. Moreover, this phosphate oxygen atom makes close contact with the face of aromatic ring 4 (see Figure 1 for the ring numbering) [the shortest distance of 3.09 Å with C_{39}], possibly through an O–H···π hydrogen-bonding (not shown in the figure), where the hydrogen atom behaves as a bifurcated hydrogen-bonding donor. These multiple interactions of the phosphate ligand with the peptide backbone, especially, the formation of a P–O–H···O (V2:4) hydrogen-bonding, may be responsible for higher affinity of the phosphate ligand toward antibiotic over a depsipeptide ligand *N*-acetyl–D-Ala–D-lactate that may suffer from V2:4 O···O (ester oxygen of the ligand) electrostatic repulsion when it binds to the peptide backbone of antibiotic. In the AcDA complex, the AcDA ligand is well fitted into the binding pocket by forming four conventional hydrogen bonds with the antibiotic backbone to orient the D-Ala methyl group so as to make close contacts with the front edge of ring 2 [3.85 Å to C_{20}], the face of ring 4 [the perpendicular distance of 3.78 Å], and the chlorine atom of ring 6 [3.56 Å] (See Figure 6b for reference and Table S-3). These multiple hydrophobic interactions could be responsible for the higher binding-affinity observed for AcDA, comparing with, for example, that of *N*-acetylglycine [values of the binding-affinity obtained by NMR measurements are 300 and 80 M^{-1}, respectively[27]].

Table 3 also shows that in crystals, there seems no apparent correlation between the tightness due to the antibiotic–ligand hydrogen-bonding and the molecular size.

Structure of Face-to-Face Arranged Self-Dimer. In the crystal lattice, two V1 molecules form a face-to-face arranged self-dimer V1–V1′ with a crystallographic 2-fold axis that passes through the water molecule located at the center of the dimer-interface, as shown in Figure 5. V1 and V1′ molecules are connected to each other directly by a pair of hydrogen bonds between the carbamoyl nitrogen of Asn residue 3 and the carbonyl oxygen of residue 4 of its dimer partner across the 2-fold axis [V1:3 $N^{\delta 2}$···V1′:4 O = 2.84 Å for the phosphate complex and 2.90 Å for the AcDA complex] and in addition, indirectly by two pairs of water-mediated hydrogen-bondings [V1:4 O···O_W···V1′:4 O; V1:7 O_{79}···O_W···V1′:7 O_{79}]. The side-chain of the C-terminal Leu residue of V1 (or V1′) molecule locates at the hydrophobic pocket of V1′ (or V1) molecule, making multiple interactions involving a close contact with the methyl substituent C_{5M} of vancosamine of the dimer partner [V1:1 C^{γ}···V1′:Van C_{5M} = 4.14 and 4.25 Å for the phosphate and AcDA complexes, respectively]. All of these intermolecular interactions could contribute to the enhancement of the formation as well as the stabilization of the face-to-face arranged V1–V1′ dimeric structure. A question arises here why V1 but not V2 molecule forms the face-to-face arranged self-dimer. A model-building study (using the the program ProFit[25] by imposing the aglycone of V2 monomer on that of V1

Table 3. Hydrogen-Bonding Distances (Å) between Vancomycin[a)] (V) and Ligand (L) Molecules in Crystal Structures of Vancomycin Complexes

Vancomycin	Ligand	OAc[b)]	AcG[b)]	DLac[b)]	AcDLac[b)]	Phosphate[b)]	AcDA[b)]	NAAA[c)]	DALAA[d)]
V1:2 N	L: OXT							2.79	2.79
V2:2 N	L: OXT	2.81	2.79	2.81	2.82	2.98	2.77	2.85	2.76
V1:3 N	L: O							2.80	2.99
V2:3 N	L: O	2.88	3.01	2.90	2.92	2.83	2.88	2.92	2.96
V1:4 N	L: O							2.86	2.81
V2:4 N	L: O	2.91	2.98	2.93	2.93	2.90	2.86	2.83	2.77
V1:4 O	L: N							2.84	2.98
V2:4 O	L: N(O[e),f)])		2.94	2.77[e)]		3.15[f)]	2.90	2.89	2.90
V1:7 N	L: O							2.88[g)]	2.88
V2:7 N	L: O							2.87	2.88

a) Vancomycin takes two types of monomers in which the vancosamine sugar lies over the ligand-binding pocket in the V1 monomer, while the glucose occupies the corresponding position in the V2 monomer (see the text). b) No ligand is bound to V1. c) The NAAA complex involves 6 independent V–L pairs. Average values are given for 3 V1–L and 3 V2–L pairs. d) The DALAA complex involves 6 independent V–L pairs. Average values are given for 4 V1–L and 2 V2–L pairs. e) Hydroxy oxygen of DLac ligand. f) Protonated oxygen of phosphate ligand. g) Average value is given for 2 V1–L pairs.

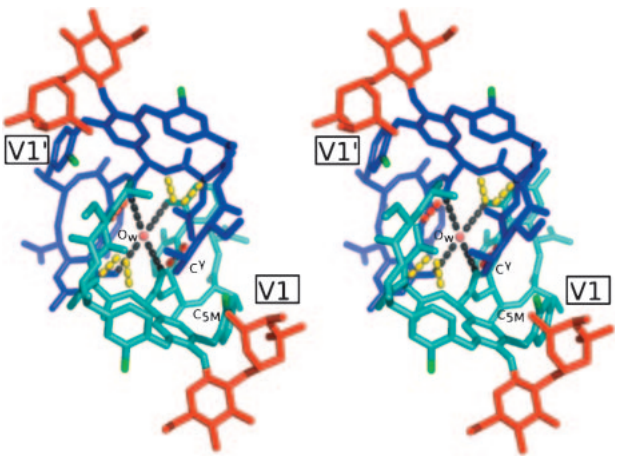

Figure 5. Stereoview showing the face-to-face arranged self-dimer V1–V1′ in the AcDA complex. The dimeric structure is stabilized by direct or water-mediated hydrogen bonds between V1 and V1′ monomers, shown in red or gray dotted lines, respectively, across a crystallographic dyad axis passing through the water molecule (pink sphere), the former being a pair of V1:3 $N^{\delta 2}$···V1′:4 O hydrogen bonds and the latter being two pairs of V1:4 O···O_W···V1′:4 O and V1:7 O_{79}···O_W···V1′:7 O_{79} hydrogen bonds. Note that the Leu side-chain occupies the ligand-binding site of its dimer partner.

monomer) shows that when V2 molecules form the face-to-face arranged self-dimer V2–V2′, the glucose sugar locates at a remote position from the Leu side chain of its dimer partner (as shown in Figure S-4), thereby making hydrophobic interaction less effective [the nearest interatomic V2:1 C^{γ}···V2′:Glu $C_{5'}$ distance of 5.71 Å for the AcDA complex].

Comparison of the Two AcDA Complexes with Tetragonal and Triclinic Crystal Forms. The triclinic AcDA complex[12] involves four independent vancomycin monomers (two independent back-to-back dimers), each of which incorpotates a ligand. Thus, the ratio of vancomycin:ligand is 1:1 in the triclinic form, while it is 2:1 in the present tetragonal form. The most interesting structural feature in the triclinic form is the first observation that vancomycin forms the ligand-mediated face-to-face arranged dimer but in this case, two incorporated ligands do not come into any direct contact. A modified ligand-mediated face-to-face dimeric structural motif has subsequently been observed in complexes with longer ligands (high-affinity ligands), such as a balhimycin complex[5] with L-Lys–D-Ala–D-Ala, or a degluco-balhimycin complex[5] with L-Ala–D-Glu–γ-L-Lys–D-Ala–D-Ala and vancomycin complexes with NAAA[6,7] and DALAA,[6] where the two incorporated ligands in the binding pockets are further self-associated by forming N–H···O hydrogen bonds between peptide backbones. This ligand-mediated face-to-face oligomerization is of special interest in that, as Scheldrick et al. have argued,[5] such a structural motif may provide a realistic model for the prevention of cell-wall crosslinking by antibiotic binding. Detailed comparison between the two forms is not possible since neither PDB nor CCDC data are available for the triclinic form, and thus in this study, for referring to the data of the AcDA complex, we exclusively deal with the present tetragonal form.

Non-Equivalence in the Ligand-Binding Affinities at the Two Binding Sites in the Back-to-Back Arranged Dimer. We now try to address a question for the absence of ligand at the binding pocket in V1 monomer in the present and other low-affinity ligand complexes, by examining the ligand-binding affinity at the two binding sites in V1- and V2-type monomers, where as noted above, vancosamine locates over the ligand-binding pocket in the V1 monomer while glucose occupies the corresponding position in the V2 monomer. A comparison of the tightness of the antibiotic–ligand (L) interface at the two binding sites in V1- and V2 monomers in the NAAA[6] and DALAA[6] complexes, where both sites are ligand-bound, shows no significant difference between the corresponding hydrogen-bonding distances at the two binding sites (Table 3). The only exception is for the V:3 N···L:O hydrogen bond in the NAAA complex in which the V:3 N···L:O distance [2.80 Å] in V1 monomer is shorter than that

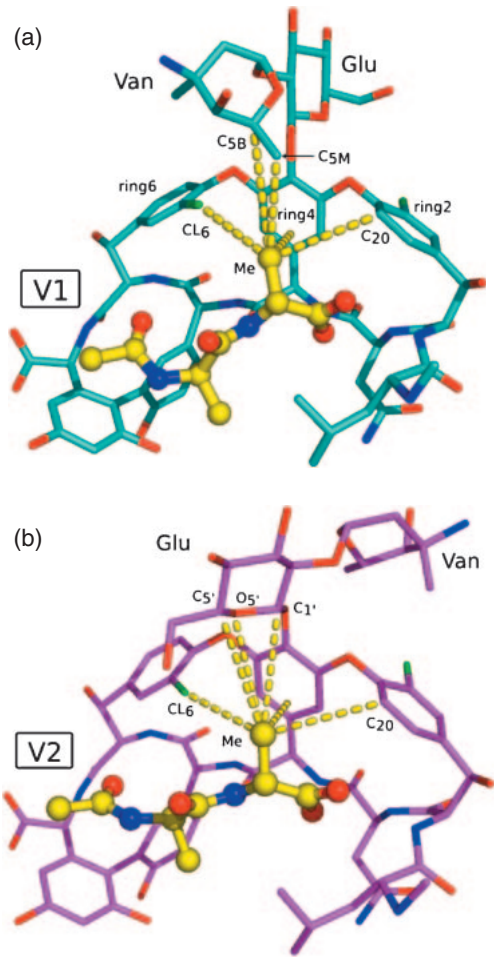

Figure 6. Multiple hydrophobic contacts between D-Ala methyl group of the ligand and the antibiotic molecule for V1 monomer (a) and V2 monomer (b) in the NAAA complex,[6] drawn with dotted lines.

[2.92 Å] in V2 monomer, whereas the corresponding distance is comparable to each other in V1 and V2 monomers of the DALAA complex. Thus the absence of the ligand in V1 monomer in these low-affinty ligand vancomycin complexes is not explicable in the term of the peptide-backbone–ligand affinity, which can be estimated to be essentially equivalent between the two sites.

On the other hand, the sugar–ligand interaction seems to be less favorable for V1 monomer than for V2 monomer, since, in the NAAA and DALAA complexes, very short close contact [distributed from 3.42 to 3.82 Å] is observed in V1 monomer between the methyl side-chain group of the terminal D-Ala residue of the ligand and the methyl substituent (C_{5M}) of vancosamine (Figure 6a and Table S-3). This indicates that the methyl–methyl close contact may suffer from considerable steric hindrance, judged from the radius of the methyl group of 2.0 Å.[28] On the other hand, in V2 monomer, multiple hydrophobic contacts occur between the D-Ala methyl group of the ligand and the edge of glucose (ring-atoms $C_{1'}$ or $O_{5'}$) (Figure 6b) [interatomic distances in the normal range of 4.03–4.59 Å (Table S-3)]. This may contribute to the stabilization of the antibiotic–ligand interface.

Possible Scenarios for the Complex Formation. In the low-affinity ligand complexes, a model-building study (using the program Profit[25]) shows that sugar–ligand steric constraint is negligible when the ligand binds to V1 monomer [for example, in the phosphate complex, the calculated nearest V1:Van C_{5M}···O (phosphate ligand) contact is 4.45 Å]. Accordingly, the absence of the ligand in V1 is most probably due to an inherent property of vancomycin to form a face-to-face arranged V1–V1′ self-dimer, where each ligand-binding site is occupied by the side-chain of the Leu residue of its dimer partner, thereby preventing the ligand from binding to V1 (Figure 5). On the other hand, the absence of the ligand in V1 in the present AcDA complex is somewhat surprising since both sites are occupied in the triclinic vancomycin–AcDA complex.[12] The formation of these two different crystal forms may be interpretable by considering the crystallization processes associated with the crystallization conditions. With the triclinic AcDA complex (crystallized from 27 mM antibiotic and 0.1 M AcDA[12]), we assume that a back-to-back dimer may form at first, followed by the ligand binding to V2 due to the lower ligand-binding affinity toward V1 than V2. As a next step, the ligand binding to V1 (of the V1–V2 dimer where the ligand-binding site of V2 is occupied) and the V1–V1′ self-dimerization (of two V1–V2 dimers with V2 being ligand-bound) may compete with each other, and as a result, since concentrations are higher for free-ligand than V1–V2 dimer-species (with V2 being ligand-bound) by at least twice, the ligand binding to V1 overcomes the V1–V1′ self-dimerization to yield a vancomycin complex with both sites occupied. On the other hand, with the present AcDA complex (crystallized from equimolar (50 mM) antibiotic and *N*-acetyl–D-Ala–D-lactate), the hydrolysis of *N*-acetyl–D-Ala–D-lactate (to give AcDA) takes some time during which the V1–V1′ self-dimer forms at first, and once this is formed, due to the sugar–ligand repulsive close contact noted above, the ligand-binding affinity of AcDA toward V1 is not enough to displace the side-chain of the Leu residue locating at the ligand-binding site.

On the other hand, for high-affinity ligands, the formation of a back-to-back arranged V1–V2 dimer and the ligand binding to both sites may cooperatively proceed, and V1–V2 dimers subsequently self-associate by forming hydrogen bonds between the two antiparallel running ligands to give a ligand-mediated face-to-face arranged oligomer, as observed in the NAAA[6,7] and DALAA[6] complexes.

Conclusion

Despite many trials under a number of crystallization conditions, co-crystallization of vancomycin and *N*-acetyl–D-Ala–D-lactate (as a cell-wall precursor analog) has failed. We propose that, since *N*,*N*′-diacetyl–L-Lys–D-Ala–D-lactate does bind to vancomycin,[6] the third Lys residue from the C-terminus of the ligand is necessary as a minimal set for the complex formation with the vancomycin-resistent precursors terminating in –D-Ala–D-lactate, though we are aware that more direct and quantitative data on the affinity of vancomycin toward both *N*-acetyl–D-Ala–D-lactate and *N*,*N*′-diacetyl–L-Lys–D-Ala–D-lactate are indispensable to confirm our hypothesis.

Both the present phosphate and AcDA complexes belong to a family of low-affinity ligand complexes, where two vanco-

mycin molecules form a back-to-back arranged dimer V1–V2 with only one of the two ligand-binding sites occupied by a ligand in V2. In this study, we have found that (**i**) when the high-affinity ligand binds, three structural factors (hydrogen-bonding interactions between the two peptide-backbones, hydrophobic interactions between the vancosamine sugar and the cross-linked ring 6, and hydrophobic edge-to-face ring–ring interactions between cross-linked rings 4 and 6) could enhance the stabilization of the back-to-back dimer-interface to some extent, and (**ii**) the ligand-binding affinity between the two binding sites in the back-to-back arranged dimer may be less for V1 monomer than V2 monomer due to the sugar (V1:Van C_{5M})···ligand (Me group of D-Ala) steric constraint. The absence of the ligand binding to V1 in the low-affinity ligand complexes is most likely due to the formation of the face-to-face arranged self-dimer V1–V1′, where the side-chain of the Leu residue of V1 (V1′) locates at the ligand-binding pocket of V1′ (V1) as a surrogate ligand. The suger–ligand steric constraint may be an additional reason for the absence of the ligand in V1 of the present AcDA complex. In this context, solution studies on whether the formation of the face-to-face arranged self-dimer V1–V1′ is an inherent nature of vancomycin for low-affinity ligands and especially when ligand is free, and whether there exists any difference in the ligand-binding affinity between the two binding sites in the back-to-back arranged dimer when AcDA binds, are of special interest and remain to be undertaken.

Experimental

Synthesis of *N*-Acetyl–D-Ala–D-Lactate. *N*-Acetyl–D-Ala–D-lactate was prepared according to the literature.[29] General information: Mp is uncorrected. NMR spectra were recorded on a JEOL GSX-270 spectrometer. ^{1}H NMR and ^{13}C NMR chemical shifts are reported in δ-values based on internal tetramethylsilane ($\delta_H = 0$), or solvent signal ($CDCl_3$ $\delta_C = 77.0$) as reference unless otherwise indicated. IR spectra were recorded on a HORIBA FT-720 Fourier-transform infrared spectrometer. Flash silica gel column chromatography was carried out on Merk Kieselgel 60 (230–400 mesh), Art. Nr. 9385. Optical rotations were measured on a Rudolph Research Analytical AUTOPOL V polarimeter, and $[\alpha]_D$-values are given in units of 10^{-1} deg cm^2 g^{-1}.

Synthesis of Benzyl *N*-Benzyloxycarbonyl–D-Alanyl–D-Lactate (Benzyl *N*-Z–D-Ala–D-Lactate): To an ice-cooled solution of *N*-Z–D-Ala (3.80 g, 17.0 mmol), benzyl D-lactate (3.07 g, 17.0 mmol; prepared by the iodine-catalyzed transesterification[30] from methyl D-lactate and benzyl alcohol) and *N*,*N*-dimethylaminopyridine (DMAP) (2.09 g, 17.1 mmol) in dry CH_2Cl_2 (100 mL) was added dropwise a solution of dicyclohexylcarbodiimide (DCC) (3.89 g, 18.9 mmol) in dry CH_2Cl_2 (20 mL), and the reaction mixture was stirred for ca. 22 h at rt. During this time, an additional amount of *N*-Z–D-Ala (194 mg, 0.867 mmol) and *N*,*N*-dimethylaminopyridine (DMAP) (108 mg, 0.887 mmol) were supplied. The mixture was filtered through a pad of Celite. The filter cake was eluted with EtOAc. The filtrate was washed successively with saturated $NaHCO_3$ aq., 0.5 M HCl, saturated $NaHCO_3$ aq. and brine, and dried ($MgSO_4$), and concentrated in vacuo. The residue was purified by flash column chromatography (hexane:EtOAc = 11:1) to give *N*-Z–D-Ala–D-lactic acid benzyl ester (6.32 g; 96% yield) as a colorless oil; $[\alpha]_D^{26.4}$ +36.7° (*c* 1.15, $CHCl_3$); ν_{max} (neat)/cm^{-1} 3346, 1749, 1724, 1525, 1456, 1252, 1211, 1174, 1097, 1072, 752, 698; ^{1}H NMR (270 MHz, $CDCl_3$): δ 7.41–7.24 (m, 10H), 5.38–4.99 (m, 5H), 5.27 (br d, $J = 7.3$ Hz, 1H), 4.43 (dq, $J = 7.3$, 7.3 Hz, 1H), 1.52 (d, $J = 7.1$ Hz, 3H), 1.41 (d, $J = 7.3$ Hz, 3H); ^{13}C NMR (67.8 MHz, $CDCl_3$): δ 172.5, 170.1, 155.6, 136.2, 135.1, 128.6, 128.5, 128.2, 128.14, 128.05(2), 69.2, 67.1, 66.9, 49.3, 18.4, 16.7; Anal. Calcd for $C_{21}H_{23}NO_6$: C, 65.44; H, 6.02; N, 3.63%. Found: C, 65.21; H, 6.12; N, 3.82%.

Synthesis of *N*-Acetyl–D-Ala–D-Lactate: To a solution of benzyl *N*-Z–D-Ala–D-lactate (4.00 g, 10.4 mmol) in MeOH (25 mL) was added a suspension of 10% Pd–C (1.42 g) in EtOAc (14 mL). The reaction mixture was stirred vigorously for 1.5 h under H_2 atmosphere at rt. The mixture was filtered through a pad of Celite, and the filter cake was eluted with MeOH and distilled water. The filtrate was concentrated in vacuo. To an ice-cooled solution of the residue was added successively $NaHCO_3$ (1.36 g, 16.2 mmol) and acetic anhydride (1.50 mL, 15.9 mmol), and the reaction mixture was stirred for ca. 20 h at rt. To the mixture was added 3 M HCl (ca. 5 mL) at 0 °C, and the resulting mixture was extracted several times with EtOAc. The extract was dried ($MgSO_4$), and concentrated in vacuo. The residue was purified by recrystallization from EtOAc–hexane to give *N*-acetyl–D-Ala–D-lactate (1.25 g, 59%) as colorless rods; mp 147–149 °C; $[\alpha]_D^{24.8}$ +124° (*c* 0.730, H_2O); ν_{max} (KBr)/cm^{-1} 3400, 3001, 2534, 2501, 1751, 1728, 1622, 1541, 1448, 1377, 1236, 1213, 1167, 1095, 1038, 633, 563, 484, 413; ^{1}H NMR (270 MHz, D_2O, referred to the residual signal of HOD at 4.65 ppm): δ 4.98 (q, $J = 7.1$ Hz, 1H), 4.30 (q, $J = 7.3$ Hz, 1H), 1.89 (s, 3H), 1.40 (d, $J = 7.1$ Hz, 3H), 1.32 (d, $J = 7.5$ Hz, 3H); ^{13}C NMR (67.8 MHz, D_2O, acetone as internal reference at 30.6 ppm): δ 175.3, 174.6, 174.5, 70.7, 48.9, 21.8, 16.4, 16.2; Anal. Calcd for $C_8H_{13}NO_5$: C, 47.29; H, 6.45; N, 6.89%. Found: C, 47.31; H, 6.49; N, 7.00%.

Crystallization and Data Collection. Vancomycin was purchased from Wako Junyaku and used without further purification. Crystals were grown by hanging drop vapor diffusion at room temperature. A total of thirty different reservoirs were tested in co-crystallization experiments of vancomycin and *N*-acetyl–D-Ala–D-lactate using Crystal Screen kits,[31] yielding two crystalline compounds, one being a phosphate complex and the other being an AcDA complex.

Crystallization of the Phosphate Complex under the Presence of *N*-Acetyl–D-Ala–D-Lactate at pH 6.5: The drop solution contained 2 µL of 50 mM vancomycin, 2 µL of 50 mM *N*-acetyl–D-Ala–D-lactate, and 2 µL of reservoir solution. The 500 µL reservoir solution contained 2.0 M NaCl, 0.2 M Na/K phosphate, and 0.10 M 2-(morpholino)ethanesulfonic acid (pH 6.5). Bipyramidal crystals grew to about 0.6 × 0.6 × 0.8 mm^3 in a few weeks.

Crystallization of the AcDA Complex, Derived from the Hydrolysis of *N*-Acetyl–D-Ala–D-Lactate at pH 4.5: The drop solution contained 2 µL of 50 mM vancomycin, 2 µL of 50 mM *N*-acetyl–D-Ala–D-lactate, and 2 µL of reservoir solution. The 500 µL reservoir solution contained 2.0 M NaCl, and 0.1 M sodium acetate (pH 4.5). Bipyramidal crystals grew to about 0.2 × 0.3 × 0.6 mm^3 in a few weeks.

Data Collection: One crystal was used for the data collection for each of the phosphate and AcDA complexes. The crystal was flash-cooled by a stream of cold nitrogen gas at 95 K with the addition of glycerol as cryoprotectant. Diffraction data were measured up to 1.10 Å for the phosphate complex and 0.95 Å for the AcDA complex at beam line BL38B1 at the Japan Synchrotron Radiation Research Institute (Spring-8, Hyogo). Oscillation angle and exposure time were 1.0°/frame and 15 s/frame, respectively. Integrated intensities were calculated using the

Table 4. Statistics of Crystal, Data Collection and Refinement

Ligand	Phosphate	AcDA
Contents of an asymmetric unit cell		
Vancomycin	$2 \times C_{66}H_{77}N_9O_{24}Cl_2$	$2 \times C_{66}H_{77}N_9O_{24}Cl_2$
(FW)	(2×1451.4)	(2×1451.4)
Ligand	$[HPO_4]^{2-}$	$[C_5H_8NO_3]^-$
(FW)	(96.0)	(130.1)
Ion	$3 \times Cl^-$, Na^+	$3 \times Cl^-$, Na^+
(FW)	(129.3)	(129.3)
Water molecule	23 (full) and 1 (partial)	32 (full) and 2 (partial)
Temperature/K	95	95
Wavelength/Å	0.700	0.700
Space group	$P4_32_12$	$P4_32_12$
Unit cell parameters		
a/Å	28.49(3)	28.22(3)
b/Å	28.49(3)	28.22(3)
c/Å	65.42(7)	65.69(7)
V/Å^3	53093(91)	52299(90)
Z	8	8
Vm	2.14	2.10
Solvent content/%	42.4	41.5
Resolution range/Å	14.8–1.10	28.2–0.95
Observed reflections	78896	157178
Independent reflections	11585	17050
Completeness/%	99.8	97.4
Multiplicity	6.8	9.2
R_{merge} (I)	0.069	0.063
Resolution range/Å	9.98–1.10	9.98–0.95
Reflections used for refinement	10896	15885
Cut off (σ)	4	4
Completeness/%	94.2	90.9
Final R	0.128	0.127

program MOSFLM,[32] and scaling was performed using the program SCALA[33] of the CCP4 program package. Crystal data and data collection statistics, together with refinement statistics, are listed in Table 4.

Structure Solution and Refinement. Initial models were obtained by molecular replacement (MR) with the program AMORE[34] of the CCP4 program package. As a search model, the vancomycin dimer of the PDB code 1C0R[35] was used. MR calculations with the standard protocol gave the solution with R values of 33.6% for the phosphate complex and 32.1% for the AcDA complex. The crystallographic refinements were performed with the program REFMAC5[36] of the CCP4 program package. The model was refined under chemical restrictions with a restriction file that was generated referring the library file of vancomycin, VAN.cif, of the CCP4 program suite. The electron density maps, $2mF_o - dF_c$ map, $F_o - F_c$ map, and omit map were calculated and checked by the program XTALVIEW,[37] revealing a phosphate ion in the phosphate complex or an AcDA ligand in the AcDA complex, in addition to three chloride ions, a sodium ion, and water molecules in both complexes. After a few cycles of refinement with isotropic thermal parameters, the anisotropic refinement gave the final R values of 12.8% for the phosphate complex and 12.7% for the AcDA complex. The crystallographically asymmetric unit contains two vancomycin monomers, a phosphate ion, three chloride ions, a sodium ion, 18 fully-occupied water molecules, and a half-occupied water molecule in the phosphate complex, while two vancomycin monomers, an AcDA ligand, three chloride ions, a sodium ion, 28 fully-occupied water molecules, and 2 half-occupied water molecules in the AcDA complex. In the phosphate complex, the phosphate ion exists as HPO_4^{2-} as evidenced by its molecular dimensions, in accordance with the crystallization conditions (pH 6.5). Crystallographic data have been deposited with Cambridge Crystallographic Data Centre: Deposition numbers CCDC-728179 and -728180 for the phosphate and AcDA complexes, respectively. Copies of the data can be obtained free of charge via http://www.ccdc.cam.ac.uk/conts/retrieving.html (or from the Crystallographic Data Centre, 12, Union Road, Cambridge, CB2 1EZ, U.K.; Fax: +44 1223 336033; e-mail: deposit@ccdc.cam.ac.uk).

Supporting Information

Lists of distances between disaccharides (Table S-1) and sugar–ring distances (Table S-2), at the back-to-back dimer-interface. A list of contacts between the methyl group of the D-Ala moiety of the ligand and the antibiotic at the ligand-binding site (Table S-3). Figures showing a V1 monomer (Figure S-1), V2-monomers (Figure S-2), and edge-to-face arranged rings 4 and 6 at the back-to-back dimer-interface (Figure S-3). A figure showing a model for a face-to-face arranged self-dimer V2–V2′ (Figure S-4). These materials are available free of charge on the web at http://www.csj.jp/journals/bcsj/.

References

1 D. H. Williams, B. Bardsley, *Angew. Chem., Int. Ed.* **1999**, *38*, 1172, and references therein.

2 P. Courvalin, *Antimicrob. Agents Chemother.* **1990**, *34*, 2291.

3 H. R. Perkins, *Biochem. J.* **1969**, *111*, 195.

4 D. H. Williams, M. P. Williams, D. W. Butcher, S. J. Hammond, *J. Am. Chem. Soc.* **1983**, *105*, 1332.

5 C. Lehmann, G. Bunkóczi, L. Vértesy, G. M. Sheldrick, *J. Mol. Biol.* **2002**, *318*, 723.

6 Y. Nitanai, T. Kikuchi, K. Kakoi, S. Hanamaki, I. Fujisawa, K. Aoki, *J. Mol. Biol.* **2009**, *385*, 1422.

7 P. J. Loll, A. Derhovanessian, M. V. Shapovalov, J. Kaplan, L. Yang, P. H. Axelsen, *J. Mol. Biol.* **2009**, *385*, 200.

8 C. T. Walsh, *Science* **1993**, *261*, 308.

9 N. E. Allen, D. L. LeTourneau, J. N. Hobbs, Jr., *J. Antibiot.* **1997**, *50*, 677.

10 T. I. Nicas, C. T. Cole, D. A. Preston, A. A. Schabel, R. Nagarajan, *Antimicrob. Agents Chemother.* **1989**, *33*, 1477.

11 C. T. Walsh, S. L. Fisher, I.-S. Park, M. Prahalad, Z. Wu, *Chem. Biol.* **1996**, *3*, 21.

12 P. J. Loll, R. Miller, C. M. Weeks, P. H. Axelsen, *Chem. Biol.* **1998**, *5*, 293.

13 P. J. Loll, A. E. Bevivino, B. D. Korty, P. H. Axelsen, *J. Am. Chem. Soc.* **1997**, *119*, 1516.

14 M. Schäfer, T. R. Schneider, G. M. Sheldrick, *Structure* **1996**, *4*, 1509.

15 P. J. Loll, J. Kaplan, B. S. Selinsky, P. H. Axelsen, *J. Med. Chem.* **1999**, *42*, 4714.

16 M. Kucharczyk, M. Brzezowska, A. Maciąg, T. Lis, M. Jeżowska-Bojczuk, *J. Inorg. Biochem.* **2008**, *102*, 936.

17 J. Kaplan, B. D. Korty, P. H. Axelsen, P. J. Loll, *J. Med. Chem.* **2001**, *44*, 1837.

18 M. Schäfer, E. Pohl, K. Schmidt-Bäse, G. M. Sheldrick, R. Hermann, A. Malabarba, M. Nebuloni, G. Pelizzi, *Helv. Chim. Acta* **1996**, *79*, 1916.

19 M. Schäfer, G. M. Sheldrick, T. R. Schneider, L. Vértesy, *Acta Crystallogr., Sect. D* **1998**, *54*, 175.

20 G. M. Sheldrick, E. Paulus, L. Vértesy, F. Hahn, *Acta Crystallogr., Sect. B* **1995**, *51*, 89.

21 C. Lehmann, J. É. Debreczeni, G. Bunkóczi, M. Dauter, Z. Dauter, L. Vértesy, G. M. Sheldrick, *Helv. Chim. Acta* **2003**, *86*, 1478.

22 G. M. Sheldrick, P. G. Jones, O. Kennard, D. H. Williams, G. A. Smith, *Nature* **1978**, *271*, 223.

23 R. Nagarajan, K. E. Merkel, K. H. Michel, H. M. Higgins, Jr., M. M. Hoehn, A. H. Hunt, N. D. Jones, J. L. Occolowitz, A. A. Schabel, J. K. Swartzendruber, *J. Am. Chem. Soc.* **1988**, *110*, 7896.

24 D. A. Beauregard, D. H. Williams, M. N. Gwynn, D. J. Knowles, *Antimicrob. Agents Chemother.* **1995**, *39*, 781.

25 A. D. McLachlan, *Acta Crystallogr., Sect. A* **1982**, *38*, 871.

26 R. Nagarajan, *Antimicrob. Agents Chemother.* **1991**, *35*, 605.

27 C. M. Pearce, U. Gerhard, D. H. Williams, *J. Chem. Soc., Perkin Trans. 2* **1995**, 159.

28 L. Pauling, *The Nature of the Chemical Bond*, 3rd ed., Cornell University Press, New York, **1960**, p. 260.

29 K. Nakamura, S. Nishiyama, S. Yamamura, *Tetrahedron Lett.* **1996**, *37*, 191.

30 K. Ramalinga, P. Vijayalakshmi, T. N. B. Kaimal, *Tetrahedron Lett.* **2002**, *43*, 879.

31 J. Jancarik, S.-H. Kim, *J. Appl. Crystallogr.* **1991**, *24*, 409.

32 A. G. W. Leslie, in *Crystallographic Computing*, ed. by D. Moras, A. D. Podjarny, J. C. Thierry, Oxford University Press, Oxford, **1993**, pp. 50–61.

33 Collaborative Computational Project, Number 4: *Acta Crystallogr., Sect. D* **1994**, *50*, 760.

34 J. Navaza, *Acta Crystallogr., Sect. A* **1994**, *50*, 157.

35 P. J. Loll, J. Kaplan, B. Selinsky, P. H. Axelsen, **1999**, PDB ID: 1C0R.

36 G. N. Murshudov, A. A. Vagin, A. Lebedev, K. S. Wilson, E. J. Dodson, *Acta Crystallogr., Sect. D* **1999**, *55*, 247.

37 D. E. McRee, *J. Struct. Biol.* **1999**, *125*, 156.